Multi-Physics Analysis of a Refractory Metal AC-Operated High Temperature Heater with Abaqus

C. Feist[*], and A. Plankensteiner[**]

[*] CENUMERICS, A-6020 Innsbruck, Austria, www.cenumerics.com

[**] PLANSEE SE, A-6600 Reutte, Austria, www.plansee.com

Abstract: Electrically operated high temperature furnaces and reactors are used in many industrial manufacturing processes such as sintering or single crystal growth in order to allow for the required process conditions. In view of their outstanding characteristics refractory metals are ideally suited as materials for the resistive heating elements. Nevertheless, significant and life-time-limiting irreversible deformations of these elements can be frequently observed which are assumed to be caused by a combination of temperature expansion, electromagnetic forces, and high temperature creep effects. In order to study this undesired behavior, a multi-physics model of a particular three-phase AC heating element of a sintering furnace is formulated and implemented within Abaqus. It accounts for the primary involved coupled physical mechanisms such as the harmonic electrical field problem, the thermal problem governed by Joule's law, thermal expansion, high temperature creep and harmonic forces caused by the electromagnetic field along with field dependent constitutive behavior. Since in general solving the fully coupled problem on a 3D domain is computationally demanding and Abaqus lacks functionality in the field of electromagnetism, a semi-analytical approach for consideration of time-harmonic electromagnetic forces within mechanical analysis is developed in the present work. The model implemented as a user-defined extension for Abaqus is computationally very attractive since it avoids discretization of the medium surrounding the heater. Furthermore, some aspects of modeling coupled physical problems of different characteristic time-scale are briefly discussed. Results from application of the model are in good qualitative agreement with in-situ observations and confirm the relevance of considering electromagnetic forces within analysis of high temperature furnaces.

Keywords: powder metallurgy, refractory metal, Tungsten, high temperature, resistive heater, three-phase, alternating current, AC, electromagnetic force, creep, multi-physics.

1. Introduction

Increasing demands with respect to functionality, durability, cost efficiency and sustainability increasingly affect almost all technical products. Both, industries with exceptionally high lead time in research and development as well as industries with pronounced time-to-market requirements are thus forced to optimize their technologies already at an early stage of development or even at a stage at which the product does not even physically exist. Prominent representatives are key technologies of the future such as the photovoltaic and LED technology, respectively. The latter are in particular driven by thermal processes for single crystal growth and in thin-film technology, respectively. High temperature furnaces and reactors with corresponding hot zones enclosing the operational space typically make use of refractory metal based heater elements and thermal

Visit the SIMULIA Resource Center for more customer examples.

shielding. Most of these furnaces are driven by resistive heating with the electric field in the heating elements introducing electromagnetic fields and corresponding electromagnetic forces. Although refractory metals are known as hardly magnetizable empirical knowledge of the past indicates lifetime limitations of the heater elements due to irreversible deformations assumed to be mainly induced by magnetic forces. Therefore, it is of primary practical importance to evaluate the overall behavior of the heater assembly of high temperature furnaces in a more generalized framework by accounting for all relevant physical mechanisms.

Refractory metals such as Molybdenum (Mo) and Tungsten (W) are widely used in high temperature applications. This is primarily due to their outstanding combination of thermo-physical and mechanical material characteristics such as high density, low coefficient of thermal expansion, and high rupture as well as creep strength even at highest temperatures. These materials exhibit a good machinability and are available e.g. as semi-finished products such as sheets, bars, and wires. For instance, in the photovoltaic and LED industry Mo and W materials are typically used for all parts within the hot zone of e.g. high temperature furnaces for consolidation and crystal growth purposes or high temperature reactors in the coating industry. Such furnaces and reactors are operated at temperatures of 2,000°C and above within the hot zones requiring an adequate thermal insulation (e.g. radiation shields).

Within classical furnace and reactor engineering the design of components such as heaters has been based on isolated assessments of the primary involved physical mechanisms with explicit assumptions regarding their mutual interactions. However, for high temperature furnaces and reactors consideration of lifetime limiting factors become of increasing importance requiring a more comprehensive multi-mechanism based modeling approach to be used during the design-stage. For instance, long-term deformations of heater elements may lead to the formation of cracks within the branches of these elements or to electric short-circuits between individual heater elements. Assessing the risk of these effects requires a coupled multi-physics modeling approach such as the one developed within the present work.

2. High temperature three-phase AC operated furnace

2.1 Description of considered heater

For sintering parts produced via the powder metallurgical production route high temperature electrically operated furnaces of resistive heating type are commonly employed. To this end, a cylindrical heating element enclosing the sintering part is mounted within a cylindrical water-cooled steel containment. Between heating element (furthermore simply called heater) and containment a series of heat-shields is arranged. Depending on the geometrical dimensions of the sintering part different sizes of furnaces and heaters are used. For what follows a furnace equipped with a heater of app. 900 mm in diameter and 1800 mm in height will be considered (Figure 1a).

The heater is operated using three-phase alternating current (AC) and is part of a star-type circuit. To this end it consists of three individual cylindrical heater-segments each with an angle of aperture of app. 117° resulting in a gap between adjacent segments of app. 20 mm in width. The segments made from 2 mm W sheets serve as the primary resistive heating elements. On their bottom end the segments are flanged to water-cooled electrodes made from copper over a height of app. 200 mm. Three conventional AC transformers are employed as power-supply each connected to two neighboring heater-segments (Figure 1b). In order to ensure a symmetrical three-phase AC circuit the transformers are controlled to provide an identical frequency of $f = 50$ Hz, a constant electrical current amplitude and phase-offset of 120°. On the other hand, the star-type circuit is established using a neutral ring (Figure 1) connecting the three segments at their top over a height of app. 200 mm. The ring consists of two Mo sheets riveted to the outer and inner surface of the heater-segments resulting in a composite cross-section in this region. It is noteworthy that the neutral ring cannot be considered as a star-point or neutral point in a discrete manner, but rather fulfills the neutrality condition in an integral manner.

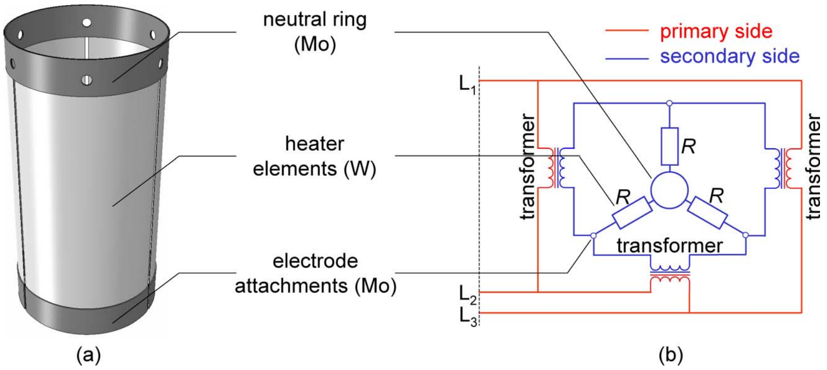

Figure 1. (a) Schematic sketch of heater of high temperature furnace, (b) circuit diagram.

From a mechanical point of view the heater is fully constrained at its bottom by means of its quasi-rigid electrodes. However, in order to avoid long-term axial high temperature creep deformations arising from dead load part of the axial load is compensated using pre-stressing devices attached to the neutral ring at six circular openings of equiangular positions (Figure 1a).

2.2 Involved physical and coupling mechanisms

2.2.1 Time harmonic electrical field problem

From a physical point of view it is the intention to exploit *Joule*'s principle of resistive heating which states proportionality of the heat produced in a resistive device to the power applied to it. The electrical power for an arbitrary transient electrical current is given as

$$P(t) = U(t) \cdot I(t) \tag{1}$$

with $U(t)$ (SI-unit: V) and $I(t)$ (SI-unit: A) as the time-dependent signals for the electrical potential (voltage) and electrical current, respectively. For purely resistive devices these quantities are found to be proportional according to *Ohm*'s law

$$U(t) = R \cdot I(t) \tag{2}$$

with the time-invariant electrical resistance R (SI-unit: Ω) defined from the material's specific electrical resistivity ρ (SI-unit: Ωm) and the resistor's cross section area A and length l as

$$R = \rho \frac{l}{A} . \tag{3}$$

For voltage and current modulated by sine-type signals of frequency f and phase-angle φ as

$$X(t) = \hat{X}\sin(\omega t - \varphi) \tag{4}$$

with $\hat{X}$ as the signal's amplitude and $\omega = 2\pi \cdot f$ as its angular frequency the signal's *root mean square* (RMS) or *effective* value X_{RMS} (furthermore simply: X) can be put in relation to the signal's amplitude as (Grote, 2007)

$$X_{RMS} = \sqrt{\frac{1}{T}\int_{t=0}^{T} X^2(t)\,dt} = \frac{1}{\sqrt{2}}\hat{X}\ . \tag{5}$$

Though time-harmonic signals could be expressed more conveniently using complex-type *phasors* (Grote, 2007), real-valued notation is kept within the present work this way allowing usage of Abaqus for the purpose of numerical simulation.

Using RMS-values for voltage and current signals of the same frequency and introducing the phase-offset $\Delta\varphi = \varphi_U - \varphi_I$, the expression for the electrical power in Eq. (1) reads

$$P(t) = U(t)\cdot I(t) = U\ I\cos(\Delta\varphi) - U\ I\cos(2\omega t - \varphi_U - \varphi_I) = P - S\cos(2\omega t - \varphi_U - \varphi_I) \tag{6}$$

with S as the amplitude of the *apparent power* modulated with twice the frequency of the voltage and current signals. The time-invariant *effective power* P denotes the fraction of power that is available for energy conversion such as for heating purposes. From the definition of P it is evident that RMS-values of voltage and current denote values that – when applied to an equivalent direct current (DC) circuit – produce the same amount of heat as within the AC circuit.

One of the consequences of *Ohm*'s law in Eq. (2) is synchrony of sine-type voltage and current signals expressed by identity of their phase angles $\varphi_U = \varphi_I = \varphi$ and by a zero phase-offset $\Delta\varphi = \varphi_U - \varphi_I = 0$ with the effective power in Eq. (6) simply reading as $P = U\ I$.

Configuration of the heater as a symmetric three-phase AC system requires usage of three (or an integer multiple of three) heating elements being chained through equal effective values of applied electrical current and phase-offset of $2/3\cdot\pi = 120°$, respectively. A star-type circuit is then ensured through the neutral condition $U_N(t) = U_{1N}(t) + U_{2N}(t) + U_{3N}(t)$ with $U_{xN}(t)$ as the time-dependent voltage-drops through heating segment x measured between its electrode and the neutral point N . Obviously, this is only valid for a circuit with a discrete (i.e. infinitely small) neutral point. With resistive devices of finite size neutral parts are employed fulfilling the neutral condition only in a weak, i.e. integral fashion over their volume.

2.2.2 Thermal problem

So far resistive devices only have been considered in a lumped fashion using integral quantities such as their electrical current I and electrical resistance R assuming a constant current density over their cross-section. In general, by various reasons the electrical current is distributed in an inhomogeneous fashion over the volume of a resistive device described by the electrical current density (with respect to the area perpendicular to its direction of flow) as $\mathbf{J}(\mathbf{x})$ (SI-unit: A/m²).

Using *Ohm*'s law Eq. (2) and the expression for the effective power in Eq. (6), the field of volumetric heat source $Q(\mathbf{x})$ (SI-unit: W/m³) defining the source-term for the thermal problem involving conduction and surface losses is given as

$$Q(\mathbf{x}) = \rho\, \mathbf{J}^2(\mathbf{x}). \tag{7}$$

Radiative heat loss is utilized to transmit thermal energy from the heater to the enclosed sintering part requiring a high coefficient of emissivity ε on its interior face. In order to minimize radiative losses over its outer surface special surface treatments providing a lower coefficient of emissivity together with heat-shields allowing for reflection are usually employed. The thermal state within the interior of the furnace is characterized by large temperature gradients causing thermally induced gas-flow. As a consequence, a certain amount of convective heat loss also takes place. After heating up of the furnace quasi-stationary conditions are established within its interior with respect to the fluid-flow (neglecting local turbulences), the harmonic electrical and the thermal situation. Steady state conditions will then be kept over the duration required for full sintering of the sintering part, which is in the order of magnitude of about 10 h. Since these steady state conditions are of primary interest within the present work initial and final transients will not be considered or only modeled in a simplified manner.

Thermal steady state in terms of temperature field $T(\mathbf{x})$ is solely governed through *Fourier's* equation of heat conduction by the thermal conductivity of the material which in general has to be considered a function of temperature $k = f(T)$. The time-harmonic electrical problem is defined in terms of the scalar electrical potential $U(\mathbf{x})$ and involves the electrical resistivity of the material $\rho = f(T)$. Temperature dependence of these two constitutive parameters together with dependence of the heat source Q on both scalar potential U and temperature T renders the electro-thermal problem coupled in a strong, i.e. bidirectional, way.

2.2.3 Mechanical response by thermal expansion

In addition, the temperature field $T(\mathbf{x})$ causes thermal strains within the heater leading both to mechanical displacements and stresses. If these stresses are sufficiently high to let inelastic material response take place, thermal strains may lead to irreversible deformation of the heater during steady state operation and after shut-down of the furnace. Inelastic material response can be attributed for example to simple time-independent metal-plasticity with temperature-dependent yield strength and hardening characteristics. However, it is obvious that structural parts operated at high temperatures of app. 2,000°C are more sensitive to time-dependent, i.e. viscous inelastic deformation such as from high temperature creep effects (Rösler, 2008).

Heaters are cyclically operated over their lifetime and depending on the type and intensity of inelastic deformation they can undergo mechanical shakedown after a number of cycles characterized by a stabilization of the inelastic deformation pattern. In the worse case shakedown together with an acceptable amount of inelastic deformation still allowing full functionality of the heater does not take place and sort of ratcheting can be observed. In either case functionality of the heater can be limited or even disabled by inelastic deformation of a certain amount.

However, as long as these deformations are relatively small, they will not have any significant influence on the electrical and thermal state during the operation. Hence, only weak, i.e. unidirectional coupling takes place between the electro-thermal and the mechanical problem. However, mechanical constitutive parameters such as the elastic constants, coefficient of thermal expansion and inelastic parameters in general have to be considered as temperature-dependent.

2.2.4 Electromagnetism

Along with the heating effect – desired in the context of resistive heating – electrical currents also generate a magnetic field characterized by its magnetic field intensity vector $\mathbf{H}$ (SI-unit: A/m). According to *Maxwell-Ampere*'s law and neglecting displacement currents the magnetic field intensity vector $\mathbf{H}$ is related to the electrical current density vector in differential form through

$$\nabla \times \mathbf{H} = \mathbf{J}\,. \tag{8}$$

The magnetic flux density $\mathbf{B}$ (SI-unit: T) represents the corresponding work-conjugate quantity which for a linear material is related to the magnetic field intensity by the constitutive equation

$$\mathbf{B} = \mu_0\ \mu_r\ \mathbf{H} = \mu\ \mathbf{H} \tag{9}$$

with μ as the magnetic permeability of the material with respect to magnetic fields (considered as a scalar for isotropic materials). The latter is usually expressed in terms of the dimensionless relative magnetic permeability μ_r with respect to the magnetic permeability of vacuum

$\mu_0 = 4 \cdot 10^{-7}\pi$ (SI-unit: H/m), also termed as the magnetic field constant.

On the other hand, a current-carrying conductor placed in a magnetic field experiences a mechanical force density (SI-unit: N/m³) (Rudnev, 2003) that is proportional to the electrical current and magnetic flux density

$$\mathbf{f} = \mathbf{J} \times \mathbf{B}\,. \tag{10}$$

Thus, solving for the electromagnetic field intensity $\mathbf{H}$ Eq. (8) from an external or induced current density together with the constitutive relationship Eq. (9) allows to define the force density emanating from the magnetic flux density $\mathbf{B}$. Depending on the absolute value of electrical current and the geometric configuration, electromagnetic forces can take on a significant order of magnitude and in this case have to be considered in the context of studying the mechanical response of a structure. These forces are present both for DC and AC systems. However, whereas they are time-invariant for the steady state DC case, they become time-dependent for the AC case. Since both magnetic flux density $\mathbf{B}$ and electrical current density $\mathbf{J}$ exhibit time-harmonic signals of the same frequency f, force density is modulated with frequency $2f$.

Faraday's law of induction states that the change of magnetic field with respect to time causes an induced electric eddy current of intensity $\mathbf{E}$ within the conductors placed in the magnetic field as

$$\nabla \times \mathbf{E} = -\dot{\mathbf{B}}\,. \tag{11}$$

These eddy currents – usually exploited for inductive heating (Rudnev, 2003) – also have their consequences for AC-operated resistive heating devices: due to the *skin-effect* the electrical current density is found to be higher at the skin than at the core of an AC conductor, whereas adjacent conductors tend to influence the electrical current density distribution by means of the *proximity effect*. These *current displacement effects* become more pronounced with increasing frequency and in general take place simultaneously for an assembly of AC-operated conductors. Thus, in contrast to DC systems, the electrical current density $\mathbf{J}$ becomes inhomogeneous over the cross-section of a resistor even in the case of absence of geometrically caused inhomogeneities.

From *Maxwell-Ampere*'s law Eq. (8) it becomes clear that the magnetic field intensity $\mathbf{H}$ depends on the scalar electrical potential U which by means of *Joule* heating and nonlinear constitutive behavior depends on the temperature field T. However, as long as current displacement effects are of no or only minor concern the electrical potential U does not depend on the magnetic field intensity. The same holds true for the temperature. Consequently, only weak coupling between the electro-thermal and magnetic problem is present. As far as the mechanical problem is concerned the magnetic field intensity and the electromagnetic forces depend on the spatial position of the conductors which implies that the electro-thermal problem becomes dependent on the mechanical response. However, for relatively small displacements these influences can be neglected.

3. Numerical solution to coupled physical problem

Solving the given coupled physical problem for the AC operated resistive heating device subjected to *Joule* heating, thermal expansion and electromagnetic forces in general requires the formulation of a fully coupled set of partial differential equations (PDE) for

- the time-harmonic electrical field in terms of the scalar potential U,
- the thermal steady state in terms of the temperature field T,
- the time-harmonic magnetic field in terms of the vector potential $\mathbf{A}$ (SI-unit: Wb/m) related to the magnetic flux density through $\nabla \times \mathbf{A} = \mathbf{B}$, and
- the transient displacement field in terms of the displacement vector $\mathbf{u}$.

These PDEs can be solved using a numerical method such as the finite element method (FEM). However, such a formulation of the problem exhibits several disadvantages and drawbacks:

- An electromagnetic field between conductors is only established by the presence of a magnetically permeable medium such as the fluid or gas surrounding them. Hence, solving for the magnetic field requires the medium to be part of the computational domain and discretized using an adequate mesh size, especially in the vicinity of the conductors.
- Modeling even simple geometrical components such as the heater together with the surrounding medium in a three-dimensional setting can become cumbersome and will produce large FE meshes. Conductors are usually of very limited geometric size when compared to the medium they are placed in. In order to appropriately resolve far-field conditions of the electromagnetic field the entire model is required to extend over a significant size, even if no other parts are considered outside the conductors.
- The medium serving for propagation of the electromagnetic field follows the displacements of the conductors. Hence, discretization of the medium has to be continuously adapted to the governing displacement field of the conductors and consequently must be considered within the mechanical problem. This can be accomplished using an ALE approach or by applying an artificial mechanical behavior to the medium. However, for significantly large displacements of the conductors remeshing together with solution mapping is required.

- Solving a fully coupled problem using a large FE mesh can become extremely expensive when considering the required number of degrees of freedom imposed by the set of PDEs. Therefore, such models can only be used for single re-analysis purposes of an in-situ scenario but are not useful for design purposes or parametric studies.
- Usually one is interested in results of the physical effects within the conductors rather than in those within the medium making consideration of the medium even less attractive.
- Last but not least, the FE-code Abaqus does not provide any procedure and elements for solving the electromagnetic problem. This is at least true for Abaqus up to version 6.10.

4. Analytical description of electromagnetic forces

In order to circumvent these drawbacks, a simplified model is proposed in the following. This model should allow to implicitly resolve the effects related to electromagnetic forces without the necessity to solve the fully coupled problem and to consider the medium as part of the computational domain. Thus, this approach intends to use a slim model still able to capture the dominating physical effects. Consequently, it still will remain attractive even if electromagnetism will be implemented within Abaqus as standard functionality in future releases.

The approach is based on the idea to analytically describe the electromagnetic force density $\mathbf{f}$ Eq. (10) as a function of harmonic time, spatial coordinates and electrical quantities. This function could then be applied as a volumetric force density to the mechanical model of the heater based on the results from the coupled electro-thermal analysis.

The heater element considered in the present study primarily consists of three linear and parallel conductors of considerable length which are connected by the neutral ring at their top. The cross section of each conductor is given by a circular arc of constant width and angle of aperture. Hence, the electrical current is considered to be constrained to follow the axial (z) direction with zero components of the current density in the cross-sectional (xy) plane

$$J_x = J_y = 0; \quad J_z = f(t, x, y) \tag{12}$$

From *Maxwell-Ampere*'s law Eq. (8) it then follows that the axial component of the resulting magnetic field $H_z = 0$ vanishes. By means of the isotropic constitutive relationship Eq. (9) this also holds true for the magnetic flux density $B_z = 0$. The electromagnetic force density then reads

$$\mathbf{f} = \lfloor -J_z B_y;\ J_z B_x;\ 0 \rfloor^T \tag{13}$$

with forces again acting in the cross-sectional plane only. Thus, the electromagnetic problem is fully described in a two-dimensional setting defined by the cross-section through the heater. This resembles the assumption of infinitely long parallel conductors and consequently neglects any influences violating the assumption of purely axially acting electrical currents such as any influences from the neutral ring. For the given two-dimensional setting the magnitude of the electromagnetic force density vector becomes

$$|\mathbf{f}| = \sqrt{(-J_z B_y)^2 + (J_z B_x)^2} = J_z |\mathbf{B}| . \tag{14}$$

An infinitely long straight conductor j of infinitely small cross-section placed in a medium of relative permeability μ_r generates a magnetic field with flux density at distance d given as

$$\left|\mathbf{B}_j\right| = B_j = I_j \cdot \frac{\mu_0 \mu_r}{2\pi\, d} . \tag{15}$$

From Eq. (14) and Eq. (15) then it follows that a second parallel conductor i within distance d_{ij} will at the same time experience and exert a force (related to unit length) of magnitude

$$\frac{F}{l} = I_i \cdot I_j \cdot \frac{\mu_0 \mu_r}{2\pi\, d_{ij}} \quad \text{with} \quad F_i = F_j = F , \tag{16}$$

acting along the direction defined by the vector between the conductors and with its sense of direction determined by the product of electrical currents: currents of opposing direction $I_i \cdot I_j < 0$ generate a repulsive force, currents of identical direction $I_i \cdot I_j > 0$ an attractive force.

One is tempted to extend these lumped consideration to conductors of finite and arbitrarily shaped cross-section with distance and direction vector defined by the centroids of the conductors' cross-sections. This, however, is only true in an integral fashion and does not provide any information about the force density distribution over the cross-section, which even for the case of a homogeneous current density distribution is non-uniform. For the AC-case, inhomogeneities of the electrical current density distribution due to skin-effect and proximity-effect (see Section 2.2.4) will additionally affect the distribution of the electromagnetic force density within the conductor.

However, if the lumped formulation Eq. (16) given for a conductor of infinitely small cross-section is related to infinitesimal cross-sectional elements it reads as

$$\frac{\mathrm{d}f_{ij}}{\mathrm{d}A_j} = J_i \cdot J_j \cdot \frac{\mu_0 \mu_r}{2\pi\, d_{ij}} \tag{17}$$

which defines the differential force density of dimension [F/L^5] representing the contribution of the force density from element $\mathrm{d}A_j$ to element $\mathrm{d}A_i$ with J_i and J_j as the electrical current densities for these infinitesimal elements. Defining distance d_{ij} as the norm of the distance vector between the 2D coordinates $\mathbf{x}_i$ and $\mathbf{x}_j$ of the infinitesimal elements as

$$d_{ij} = \left|\mathbf{x}_i - \mathbf{x}_j\right| = \left|\Delta\mathbf{x}_{ij}\right| \tag{18}$$

and recognizing that the components of the 2D force density vector can be obtained by projections using the corresponding unit vectors $\mathbf{n}_{ij} = \Delta\mathbf{x}_{ij} / \left|\Delta\mathbf{x}_{ij}\right|$ allows to write the vector of the differential force density contribution Eq. (17) as

$$\frac{\mathrm{d}\mathbf{f}_{ij}}{\mathrm{d}A_j} = J_i \cdot J_j \cdot \frac{\mu_0 \mu_r}{2\pi \left|\Delta\mathbf{x}_{ij}\right|} \cdot \mathbf{n}_{ij} . \tag{19}$$

This formulation can be used to compute the infinitesimal force density of dimension [F/L³] acting on element $\mathrm{d}A_i$ from integrating over the domain of conductor j

$$\mathbf{f}_i = \int \mathrm{d}\mathbf{f}_{ij} = J_i \cdot \int_{A_j} J_j \cdot \frac{\mu_0 \mu_r}{2\pi \left|\Delta \mathbf{x}_{ij}\right|} \cdot \mathbf{n}_{ij} \; \mathrm{d}A_j \, . \tag{20}$$

Interaction between infinitesimal elements according to Eq. (20) is not restricted to elements *from different conductors* but also to different elements *within the same conductor*. Moreover, in a configuration with more than two conductors, force density at a particular point will contain contributions from multiple conductors. Thus, the expression for the force density Eq. (20) is extended by summation over all N conductors present in the domain as

$$\mathbf{f}_i = \sum_{j=1}^{N} \int \mathrm{d}\mathbf{f}_{ij} = J_i \cdot \sum_{j=1}^{N} \int_{A_j} J_j \cdot \frac{\mu_0 \mu_r}{2\pi \left|\Delta \mathbf{x}_{ij}\right|} \cdot \mathbf{n}_{ij} \; \mathrm{d}A_j \, . \tag{21}$$

It is important to note that the integrated force density contributions from elements of the same conductor are canceled, such that force equilibrium is fulfilled even for a single current-carrying conductor. However, the non-uniform force density will be non-zero even in this case. Eq. (21) becomes singular for $\Delta \mathbf{x}_{ij} = \mathbf{0}$ representing potential "self-interaction" which is unphysical since the magnetic field is known to vanish at the center of a circular conductor of finite radius and therefore must not be considered within the integration.

The formulation given in Eq. (21) can be employed to compute the force density field for conductors of geometries that can be analytically described and of known electrical current density. For the heater considered in the present work, there are $N = 3$ conducting elements and the electrical currents I_1, I_2, I_3 are uniquely determined by the three-phase star-type AC circuit with defined RMS-values and constant phase-offset. The geometry of the heater cross-section can be analytically described as a cyclically symmetric circular arc of finite thickness and given angle of aperture. Displacement of the current density over the thickness t due to the skin-effect is negligible when compared to the rectified width and radius of a heater segment. Thus, for the purpose of electromagnetic force computation, it is justified to assume a constant current density distribution over thickness t. Hence, the infinitesimal element can be expressed as $\mathrm{d}A = t \cdot r \cdot d\varphi$ with $d\varphi$ denoting an infinitesimal angular element. Together with the assumption of identical radii and thickness values in all conductors the integral Eq. (21) can be expressed as

$$\mathbf{f}_i = t \cdot r \cdot J_i \cdot \sum_{j=1}^{N} \int_{\varphi=\varphi_{0,j}}^{\varphi_{1,j}} J_j \cdot \frac{\mu_0 \mu_r}{2\pi \left|\Delta \mathbf{x}_{ij}\right|} \cdot \mathbf{n}_{ij} \; \mathrm{d}\varphi \tag{22}$$

with $\varphi_{0,j}$ and $\varphi_{1,j}$ denoting the angular limits of conductor j and $\left|\Delta \mathbf{x}_{ij}\right|$ and $\mathbf{n}_{ij}$ computed from the corresponding polar coordinates. With respect to distribution of current densities in circumferential direction as a first guess one can assume a constant distribution. In order to capture AC related current displacement effects, however, it is more realistic to assume a time- and space-varying distribution function for $J = f(\varphi, t)$ which can be defined more conveniently as

$$J(\varphi,t) = \lambda(\varphi,t) \cdot \frac{I(t)}{A} = \lambda(\varphi,t) \cdot \bar{J}(t) \tag{23}$$

where $\bar{J}(t)$ is the homogeneous current density found by *smearing* the electrical current $I(t)$ over the conductor's cross-section and $\lambda(\varphi,t)$ defines a correction factor. The latter can be estimated analytically or by means of a separate numerical analysis of the two-dimensional electromagnetic problem. However, for many problems of low frequency it is sufficient to assume $\lambda(\varphi,t) = 1$.

5. Numerical implementation using the Abaqus DLOAD interface

The expression for the electromagnetic force density $\mathbf{f} = f(t,\mathbf{x})$ as a function of time and spatial coordinates can be conveniently implemented for Abaqus using its DLOAD interface (Dassault Systèmes, 2010) as a Fortran subroutine (Intel, 2006). Since the components of the force density vector represent "body loads" of dimension [F/L³], the distributed load types BXNU and BYNU (assuming the heater-axis to be aligned to the global z -axis) are employed. During a mechanical analysis the subroutine is called for each integration point in the regions where these distributed load types are applied to, whereupon it computes the required component f_x (BXNU) and f_y (BYNU). This is accomplished by summation over all N involved heater elements and numerical integration over arc-length of each of these elements with a sufficiently large number of integration points. To this end, the reference heater geometry is passed into the subroutine as user-input together with the characteristic values of the electrical current (RMS-values and phase-angles) along with piecewise or analytical description of correction function $\lambda(\varphi,t)$ Eq. (23).

Since the geometry is described in analytical manner, computation of force density is entirely local and does not require global integration over other integration points of the FE-discretization. This is achieved by using the reference (i.e. undeformed) coordinates of point i passed into the subroutine (for geometrical nonlinear analysis the coordinates passed into the routine represent current, i.e. deformed coordinates; in this case the values passed into the routine at the very first call to the subroutine are stored in a common block array) and by trying to associate these coordinates to a particular conductor based on the user-input. Together with the current value of time t (either step or total time) this allows to compute the corresponding electrical current $I(t)$ and homogeneous current density $\bar{J}(t)$ along with the value of $\lambda(\varphi,t)$. This way, the current density Eq. (23) at point i is uniquely defined. Together with the corresponding phase angles one can determine the current densities in the remainder of the heater elements and numerical integration can be easily conducted. In order to break down the singularity related to potential "self-interaction" a numerical regularization strategy is used in the vicinity of the integration point.

It is noteworthy that conductors used in numerical integration are not necessarily required to be discretized in the FE-model, since integration is carried out over an analytically described geometry and electrical current field. Hence, this also allows to exploit all symmetries of the model: For instance the heater exhibiting three-fold cyclic symmetry of a sector of single symmetry can be modeled using a 60° segment of the heater together with appropriate boundary conditions. However, this also requires that the load pattern exhibits the same type of symmetry. For postprocessing purposes all primary quantities ($\bar{J}(t)$, $\lambda(\varphi,t)$, $J(t)$, f_x and f_y) are also computed as *user defined output variables* using the UVARM interface (Dassault Systèmes, 2010) based on the same approach. This way, load values can be easily visualized and verified. The model consisting of these two subroutines can be used with any 3D FE solid and shell discretization.

6. Application to the AC operated high temperature heater

The proposed approach allows to sequentially decouple the electro-thermal and the mechanical analysis without considering the medium as part of the computational domain. Therefore, as a first step the coupled electro-thermal problem is solved. Even though the heater exhibits a (3 x 2)-fold symmetry with respect to its geometry it is necessary to consider the entire heater since the neutral ring does not allow to define a unique equivalent DC system based on RMS values (this in fact would be possible if a discrete neutral point is present). Since Abaqus does not support a complex-valued solution of the time-harmonic AC electric field problem it is necessary to consider the problem as time-dependent. In order to capture at least all peaks of the applied currents within all three heater segments the AC period of $T = f^{-1} = 0.02$ s has to be discretized by at least 12 equally sized time increments (or an integer multiple of that). With temperature-dependence of the electrical resistivity ρ the electrical field problem becomes temperature-dependent which makes consideration of coupled shakedown necessary: A shakedown of the coupled electro-thermal problem to a stationary cyclic behavior naturally takes place after a number of AC periods when equilibrium of heat produced by *Joule* heating and surface heat losses is attained. Since a direct cyclic approach (similar to the one available for mechanical analysis) based on a *Fourier* representation of the solution over an AC period is not available for this type of analysis in Abaqus, one is forced to conduct a transient analysis over a sufficiently large number of periods in order to obtain the stationary cyclic state. Due to the requirement of sufficiently fine time-discretization over a single period this can become numerically expensive even for rather short transients, i.e. heating-up times. The time-harmonic character of the electrical problem leads to spurious oscillations in the temperature field. Though amplitudes of these oscillations are very small when compared to the absolute level of temperature for physically realistic frequencies they tend to grow with decreasing frequencies. Hence, it is not recommended to artificially "stretch" the period within the coupled electro-thermal analysis step in order to arrive at larger time increments during heating-up. Instead it is advisable to apply appropriate initial conditions for the temperature field (for instance, according to ambient temperature used in the surface radiation model) in order to speed-up the transient shakedown or to artificially adjust specific heat capacity values.

Using the coupled electro-thermal procedure in Abaqus together with surface radiation requires discretization of the heater using 3D solid elements such as DC3D8E. However, since radial field variation can be neglected for the heater elements only one element is used over the thickness. The coupled electro-thermal model accounts for temperature dependence of the electrical resistivity and thermal conductivity. Voltage-controlled electrical input according to the specifications of the transformers is used by respective boundary conditions applied to the surfaces representing the interfaces to the electrodes. In order to approximately account for water-cooling of the electrodes appropriate temperatures are prescribed on these surfaces. All remaining interior and exterior surfaces are considered to radiate against ambient conditions assuming appropriate temperatures and coefficients of emissivity, whereas convective losses are not considered within the model.

In Figure 2 distributions of the electrical potential for distinct instants during a period in the shake-down state are shown, where each state corresponds to the phase-angle of maximum electrical current in each heater element. The used color range only showing positive potential values clearly indicates that the neutral ring is also acting as a resistive element over a certain angle with the isolines of zero-potential rotating with the applied AC signal.

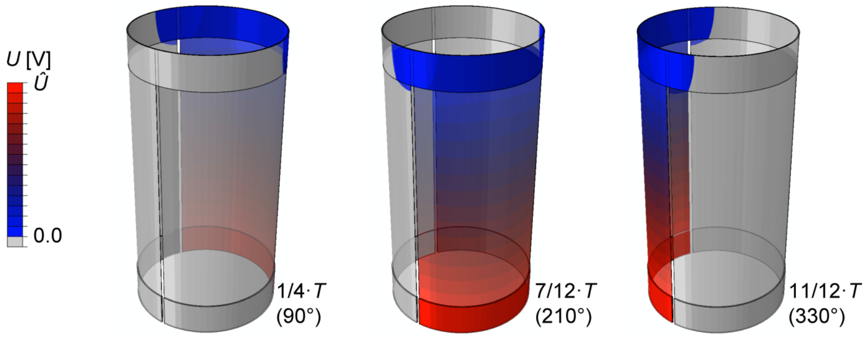

Figure 2. Results from coupled electro-thermal analysis: distribution of electrical potential for the three time-instants corresponding to the phase angles of the heater-segments.

The temperature field computed from the coupled electro-thermal analysis is then applied to a subsequent mechanical analysis which in a first step accounts for thermal expansion effects only. Considering symmetry with respect to geometry and temperature field allows the mechanical analysis to be carried out using a 60° sector of the heater with appropriate kinematic boundary conditions imposed along the planes of symmetry. In view of the small thickness of the employed W-sheets and the expected bending deformation the heater is discretized using shell elements with an appropriate number of integration points over its thickness. The neutral ring is modeled using a composite shell section. The electrodes at bottom and the lever-supports at top are modeled in a simplified manner by appropriate kinematic boundary conditions.

With respect to constitutive modeling *Mises* plasticity with temperature-dependent yield-stress and without hardening is employed. Elastic constants and the coefficient of thermal expansion are considered as temperature-dependent. Time-dependent inelastic behavior is modeled using the *Norton*-type power-law creep model (Rösler, 2008) available in Abaqus (Dassault Systèmes, 2010) again with temperature-dependent creep parameters.

Within this first mechanical analysis temperatures obtained from the electro-thermal analysis are applied as a static field in a quasi-static analysis step over a period of 10^7 s (~ 2800 h). Thus, heat-ing-up and cool-down transients for the individual operation cycles are not considered in detail. This is motivated by the fact that this first analysis step solely should serve as a baseline for the subsequent assessment of the action of electromagnetic forces. The results show that the heater experiences an expansion almost free from any distortions with maximum displacements in the order of magnitude of 0.1 mm to 1.0 mm.

In a second independent mechanical analysis the heater is subjected to the action of electromag-netic forces using the presented DLOAD subroutine using a 60° segment model of the heater (Figure 3a), where force densities are applied to the heater-segment only. Since creep can be con-sidered as the major source of inelastic deformation, significant irreversible displacements are expected upon long-term rather than upon instant force action. Hence, electromagnetic force action must be assessed in a quasi-static procedure over a period of 10^7 s. Resolving this time-scale by the AC period of only 0.02 s (responsible for time-variation of electromagnetic forces) is prohibitive in view of the computational costs. On the other hand, mechanical shakedown – allowing usage of the *direct cyclic* analysis type – in general cannot be expected. However, within the mechanical analysis it is possible to arbitrarily "stretch" the real AC period to a fictitious one as long as resolution of the total time-scale by an integer multiple of the fictitious period is guaranteed. This can be explained by the fact that the mechanical response solely depends on the accumulated time at a given load-level and is independent of the number of cycles manifesting this accumulated time. This behavior can be shown analytically using a damping element subjected to a cyclic load and has been verified in the course of this work by respective numerical experiments. This allows to consider the entire quasi-static time period by half of a single AC period (representing one electromagnetic force period). Since this does not allow to evaluate the solution at a fraction of the considered period, smaller fictitious AC periods should be chosen, if the results are to be evaluated at fractions of the total time period (for example, a total time period of 10^7 s with intermediate result requests for every 10^6 s requires discretization by five fictitious AC periods of $2 \cdot 10^6$ or ten electromagnetic force periods of $1 \cdot 10^6$, respectively).

Irrespective of the type of load application electromagnetic forces are of cyclic nature for which the time hardening power-law creep model is not perfectly well suited. However, extraction of temperature-dependent creep parameters is challenging for high temperatures even under static loading. For the given Tungsten material they have been determined in the course of an extensive experimental study. Application of the power-law creep model to the case of cyclic electromagnetic forces is furthermore justified by the fact that electromagnetic forces do not exhibit sign-reversals during the AC period, thus representing pulsating forces.

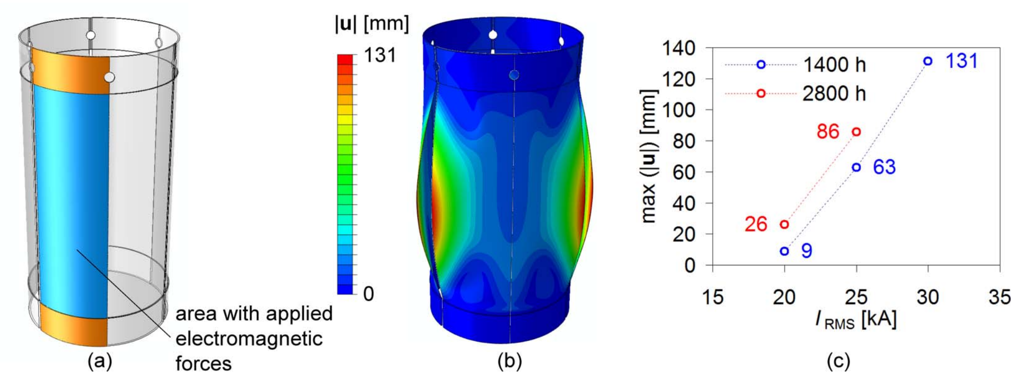

Figure 3. (a) Model for analysis considering electromagnetic forces; irreversible displacements (b) after 1400 h for 30 kA, and (c) as a function of electrical current and time.

This circumstance along with the question for analogy to the electro-thermal problem in spirit of RMS values gives rise to the question if there is sort of a characteristic electromagnetic force distribution (which in turn can be related to a characteristic electrical current state) which applied as a static (i.e. time-invariant) load will lead to the same amount of irreversible deformation as in the cyclic case. It can be shown analytically and verified by numerical models, that in fact such effective electrical current and load values can be found. The required electrical input can be related to the physical RMS value of electrical current using a modification factor. It can be shown that the latter depends on the stress exponent n of the creep model lying in the interval of $[1, 2^{0.5})$.

In Figure 3b the magnitudes of irreversible displacement are shown for the heater after the considered period of $5 \cdot 10^6$ s (~1400 h) for an effective electrical current of 30 kA. It is clearly seen that the electromagnetic forces together with high temperature creep effects can be considered responsible for large deformations disabling the functionality of the heater even for very low precision requirements. For the same current rating displacements excessively increase upon further operation leading to failure of the heater. From Figure 3c the influences both from time and electrical current input on the magnitude of irreversible displacement can be seen: the nonlinear dependencies are explained by the quadratic dependency of electromagnetic forces on the applied electrical current and the power dependency of the creep strains on the corresponding stress level.

7. Summary

In the present work a multi-physics modeling approach devoted to analyze the long-term behavior of high temperature three-phase AC heaters used for sintering is presented. Development and implementation of this model are motivated by in-situ observations of significant heater deformations which in the past qualitatively had been attributed to the action of electromagnetic forces.

Instead of using a fully coupled 3D model of the heater for solving the electric, magnetic, temperature and displacement fields requiring discretization of the medium surrounding the heater, the present approach follows an alternative strategy: the time- and space-dependent electromagnetic force densities are derived from analytical considerations for a two-dimensional representation of the heater. These relations are implemented as a user-defined extension to Abaqus.

Application of the model confirms that electromagnetic forces together with high temperature creep effects can be considered as being responsible for significant irreversible deformations upon long-term operation. In the course of this study several other aspects of load application for electromagnetic forces together with quasi-static procedures have been assessed and briefly outlined.

The proposed model is computationally very efficient since it avoids discretization of the surrounding medium. Therefore, it will keep its value even for the case that electromagnetism will be part of Abaqus standard functionality in future releases at least for cases which allow for abstractions similar to the ones applicable to the present work.

8. References

1. Dassault Systèmes, "Abaqus 6.10 Analysis User's Manual," 2010.
2. Grote, K.-H., and J. Feldhusen (Editors), "Dubbel - Taschenbuch für den Maschinenbau," 22. Auflage, Springer-Verlag Berlin-Heidelberg, 2007 (German).
3. Intel Corporation, "Intel Fortran Language Reference," 2006.
4. Rösler, J., H. Harders, M. Bäker, "Mechanisches Verhalten der Werkstoffe," 3. Auflage, Vieweg+Teubner, Wiesbaden, 2008 (German).
5. Rudnev, V., D. Loveless, R. Cook, and M. Black, "Handbook of Induction Heating," Marcel Dekker Inc., New York, 2003.